DIRECT SOLUTION

TO THE FEW-BODY INTEGRODIFFERENTIAL EQUATION

BY

MORRIS RAMANTSWANA

DIRECT SOLUTION TO THE FEW-BODY INTEGRODIFFERENTIAL EQUATION

by

MORRIS RAMANTSWANA

submitted in accordance with the requirements
for the degree of

MASTER OF SCIENCE

in the subject

PHYSICS

at the

UNIVERSITY OF SOUTH AFRICA

SUPERVISOR : PROF. G. J. RAMPHO

OCTOBER 2019

Declaration

Student : M. Ramantswana

Student No. : 5361 4593

I declare that **"DIRECT SOLUTION TO THE FEW-BODY INTEGRODIFFERENTIAL EQUATION"** is my own work and that all the sources that I have used or quoted have been indicated and acknowledged by means of complete references.

SIGNATURE DATE

Acknowledgments

I would like to thank the following individuals for encouragement and informative discussions related to this the work :

- Prof. G. J. Rampho: *University of South Africa*, SOUTH AFRICA.
  For his expert guidance and inspiration during this work.

- Dr B Mukeru, for his encouragement, guidance and availability for discussions during this work.

- M. O. Tshikororo, my partner for her patience, understanding and believing in me throughout this work.

- M. S. Ramantswana, my mother for encouragement and support.

- Members of the Department of Physics at Unisa for their support.

Summary

In this work, a direct solution to the few-body Integrodifferential equation using the Lagrange-mesh method is presented. With the Lagrange-mesh method, the few-body Integrodifferential equation is converted into a matrix eigenvalue problem for numerical treatment. The accuracy and stability of the solution is tested by calculating ground-state binding energies for few-boson systems interacting via the Ali-Bodmer, Volkov and Malfliet-Tjon (MTV) nuclear potentials for A-body systems (where $A = 4, 5, 6, 7$). A rapid convergence of the results is achieved and calculated ground-state energies are in good agreement with those available in the literature, where different approaches were used. The method is promising and could be extended to larger number of particles such as those involved in the Bose-Einstein condensates.

Keywords: Few-body systems, Hyperspherical harmonics, Faddeev approach, Integrodifferential equation approach, Adiabatic approximation, Perturbation method, Lagrange-mesh method, Lagrange basis functions, Matrix elements, Eigenvalue problem.

Contents

List of Figures

Chapter 1

Introduction

Quantum mechanical systems in atomic and nuclear physics are described using the many-body Schrödinger equation. Properties of these systems, such as binding energies, energy levels, root-mean-square radii and charge distribution are theoretically investigated through the solution of the Schrödinger equation [1, 2]. However, it is a formidable task to solve the many-body Schrödinger equation directly and exactly due to huge number of degrees of freedom which lead to many numerical complexities. Therefore, for a numerical treatment, one has to resort to simplifying approaches [3].

Generally, in literature, many-body systems are treated using two families of approaches. The first family of approaches uses correlation functions together with variational approaches to solve the many-body Schrödinger equation [3]. The second family of approach is based on assuming that the total potential of the system can be written as a sum of pairwise forces, leading the wave function of the system to be written as a sum of pairwise amplitudes that satisfy Faddeev-type equation [4]. The examples of the first family of approaches, are approximations such as Variational Monte Carlo (VMC) method [5], Diffusion Monte Carlo (DMC) and Green Function Monte Carlo (GFMC) [6], Hyperspherical harmonics expansion method (HHEM) [7] amongst other methods. On the other hand, the examples of the second family, are the Faddeev formalism [4] and the Integrodifferential equation approach (IDEA) [6].

The Hypherspherical harmonics expansion method introduced by Zernike and Brinkman in 1935 [8] and also used recently by Viviani et al [9] to treat many-body Schrödinger equation, expands the many-body Schrödinger wave function in Hyperspherical coordinates in terms of an infinite number of partial waves [10]. The expansion reduces the Schrödinger equation to a set of infinite coupled second-order differential equations [3]. The complexity of the Hyperspherical harmonics expansion formalism increases rapidly and the calculation becomes prohibitively expensive, both in memory and computer time requirements for systems with large number of particles. The number of coupled equations to be solved increases rapidly with the number of particles in the system [3]. Another disadvantage of this approach is the slow converge of the solution when a strong short range potential is used. An alternative method as powerful as the Hyperspherical harmonics expansion method is the Faddeev formalism.

The Faddeev formalism introduced in the early 1960's solves the many-body Schrödinger equation through the introduction of two-body amplitudes for pairs of interacting particles [3, 4]. The equations were introduced the same time the Hyperspherical potential harmonics was popular to resolve scattering problems [3, 4]. The formalism has been considerably used over the last few decades to study three-body exactly. Being exact, Faddeev formalism provides accurate solutions for up to only four-body system, through the Faddeev Yakubovsky formalism [11]. For systems beyond $A = 4$, the formalism requires approximations and assumptions because the equations become complex to solve. Therefore going beyond four-body systems, one has to resort to other methods such as the Integrodifferential equation approach, valid for any number of particles.

The Integrodifferential equation approach is primarily based on the expansion of many-body Schrödinger equation wave function into the Faddeev-type two-body amplitudes [10]. Subsequently the expanded Faddeev-type equations are projected on a specific two-body space to obtain, a two-variable Integrodifferential equation describing the system. The three-body Integrodifferential equation produces exactly the same results as the Faddeev equation for three body systems, this is because the three-body Integrodifferential equation is exactly identical to Faddeev equation and its structure is invariant as the number of particles A becomes large [1]. The Integrodifferential equation approach has been successfully applied in few-body calculations, in unequal mass particle systems [12], in realistic fermionic systems [3], as well as in model calculations for 16-body system. In all these applications, the energies calculated are in excellent agreement with other methods reported in literature [3].

Although mathematically sound, the numerical solution of the few-body Integrodifferential equation is cumbersome because of the kernel function involving the sum over partial waves. The few-body Integrodifferential equation has been solved by Perturbation method for $A \leq 14$ with the Baker, Volkov and MTV models which are nucleon-nucleon potentials of varying softness with Baker as the softest core and the MTV the hardest core [1, 2]. The equation has also been solved by the Adiabatic approximation for three and four nucleon ground-state systems [1, 13]. The Perturbation method solves the equations iteratively, the unperturbed differential equation is solved directly. The Adiabatic approximation technique decouples the few-body Integrodifferential equation into the radial and the angular part. The single-variable equations are then solved separately. Unfortunately, the solution of the Integrodifferential equation using Adiabatic and Perturbation methods is computationally expensive [1, 2]. Consequently, for systems such as Bose-Einstein condensates which includes more than 100 particles, one has to resort to a direct solution to the few-body Integrodifferential equation as suggested by Adams and Sofianos [3].

One of the most promising method of solving the Integrodifferential equation approach directly simpler and faster, is the Lagrange-mesh method (LMM) [14]. This method expands the Faddeev two-body amplitudes on the Lagrange basis functions. The method, has been successfully used in solving the one-dimensional Schrödinger equation in literature [14]. The Lagrange-mesh method is both accurate and efficient and allows us to choose large basis functions to achieve accurate results which is not the case with other variational methods. Also unlike with other variational approximation methods, the Lagrange-mesh method uses orthonormal Lagrange functions which vanish at all mesh points, but one. To this end, the Lagrange-mesh method gives simple analytical expressions for the matrix elements of the Hamiltonian of the system. The method generates the most accurate wave functions and energies with Gauss quadrature as in the original variational method with an exact computation of the matrix elements of the Hamiltonian with ease. In all cases, the calculations are much easier and faster than in many traditional methods in literature [14, 15].

The main objective of this work is to solve directly the Integrodifferential equation, using the Lagrange-mesh method. To this end, the Faddeev-type two-body amplitudes are first expanded on the Lagrange-mesh basis functions. The substitution of this expansion into the few-body Integrodifferential equation results in an eigenvalue problem, which is solved numerically. The accuracy of the solution is tested by calculating the ground-state energies for A-body ($A = 4, 5, 6, 7$) nuclear systems interacting, via two-body interactions such as the alpha-alpha Ali-Bodmer and nucleon-nucleon Volkov as well as the Malfliet-Tjon (MTV) potentials. The results will be compared with those available in the literature.

The dissertation is structured as follows: In Chapter 2, we briefly discuss the few-body Integrodifferential equation approach. Starting from the expansion of the many-body wave function into Faddeev-type two-body amplitudes, we discuss the mathematical derivation leading to the few-body Integrodifferential equation. In Chapter 3, the principles of Lagrange-mesh method are presented, where different Lagrange basis functions employed in this work are discussed. The results are presented and discussed in Chapter 4, with concluding remarks in Chapter 5.

Chapter 2

Few-body Integrodifferential equation approach

2.1 Background

In this chapter, we discuss the mathematical derivation of the few-body Integrodifferential equation. The few-body Integrodifferential equation, valid for any number of particles is derived using a chain of Jacobi coordinates for unequal mass particles. These coordinates are used to introduce hyperspherical coordinates and also eliminate the center of mass motion. The set of Jacobi coordinates is [12, 16]:

$$\left.\begin{aligned}
\boldsymbol{\zeta_N} &= \left[\frac{2Am_1m_2}{M(m_1+m_2)}\right]^{1/2}(r_2-r_1) \\
\boldsymbol{\zeta_{N-1}} &= \left[\frac{2A(m_1+m_2)m_3}{M(m_1+m_2+m_3)}\right]^{1/2}\left(r_3-\frac{m_1r_1+m_2r_2}{m_1+m_2}\right) \\
&\vdots \\
\boldsymbol{\zeta_{N-i+1}} &= \left[\frac{2A(\sum_{j=1}^{i}m_j)m_{i+1}}{M\sum_{j+1}^{i+1}m_j}\right]\left(r_{i+1}-\frac{\sum_{j=1}^{i}m_ir_i}{\sum_{j=1}^{i}m_i}\right) \\
&\vdots \\
\boldsymbol{\zeta_1} &= \left[\frac{2A(M-m_A)m_A}{M^2}\right]\left(r_A-\frac{\sum_{j=1}^{A}m_jr_j}{M-m_A}\right)
\end{aligned}\right\}, \tag{2.1}$$

where m_i is the mass of particle i and

$$M=\sum_{j=1}^{A}m_j \tag{2.2}$$

is the total mass of the system. The center of mass in Jacobi coordinates is represented by [12]

$$\boldsymbol{R} = \frac{1}{M}\sum_{j=1}^{A} m_j r_j, \tag{2.3}$$

where A is the number of particles and $N = A - 1$. The hyperradius r which is invariant when there is an exchange of particles, is given by [12, 16, 19]

$$r = \left[\frac{2}{A}\sum_{i=1}\boldsymbol{\zeta}_j^2\right]^{1/2} \tag{2.4}$$

for particles with equal mass, and written as [12]

$$r = \left[\frac{2A}{M}\sum_{i\leq j\leq A} m_i m_j r_{ij}^2\right]^{1/2} \tag{2.5}$$

for particles with unequal mass. The kinetic energy operator $\hat{T}$, which also does not change when the particles are interchanged, is written as [12]

$$\hat{T} = -\frac{\hbar^2 A}{M}\sum_{j=1}^{N}\nabla_{\boldsymbol{\zeta}_j}^2 - \frac{\hbar^2}{2M}\nabla_{\boldsymbol{R}}^2, \tag{2.6}$$

where

$$\hat{T}_{internal} = \frac{\hbar^2 A}{M}\sum_{j=1}^{N}\nabla_{\boldsymbol{\zeta}_j}^2 \tag{2.7}$$

and

$$\hat{T}_{cm} = \frac{\hbar^2}{2M}\nabla_{\boldsymbol{R}}^2 \tag{2.8}$$

is the center of mass kinetic energy operator. The angular coordinates over the hypersphere are described by spherical coordinates (θ_i, φ_i) of each vector $\boldsymbol{\zeta}$ and hypersperical coordinates ϕ_i. Therefore, the Jacobi coordinates are related to the hypersperical coordi-

nates as follows [12, 19]

$$\left.\begin{aligned} \boldsymbol{\zeta_N} &= r\cos\phi_N, \\ &\vdots \\ \boldsymbol{\zeta_{N-1}} &= r\sin\phi_N\cos\phi_{N-1}, \\ &\vdots \\ \boldsymbol{\zeta_i} &= r\sin\phi_N\ldots\sin\phi_{i+1}\cos\phi_i, \\ \boldsymbol{\zeta_1} &= r\sin\phi_N\ldots\sin\phi_2 \qquad (\phi_1 = 0) \end{aligned}\right\}. \tag{2.9}$$

The angular components of these coordinates represent a set of $3N-1$ coordinates describing the position of a point on the unit hypersphere $r = 1$. We now define the surface element $d\Omega$ in the $(D-3)$-dimensional using equation 2.9 as [19]

$$d\Omega = d\omega_1 \prod_{j=2}^{N} (\sin\theta)^{3j-4}\cos^2\theta_j d\theta_j, \tag{2.10}$$

where $D = 3N$, Ω is the hyperangles of particles considered, $\omega \equiv \omega_N$ and $\theta = \theta_N$. The surface element $d\Omega$ can also be defined as

$$d\Omega = (\sin\theta)^{D-4}\cos^2\theta d\theta d\omega d\Omega_{N-1}. \tag{2.11}$$

Using the surface element $d\Omega$ in $(D-3)$-dimensional space together with the hyperradius r, we define the volume element in the same space as [19]

$$d^D = r^{D-1} dr d\Omega. \tag{2.12}$$

If $z = \cos 2\theta$ (where $0 \leq \theta \leq \pi/2$), therefore [19]

$$\cos\theta = \sqrt{(1+z)/2} \tag{2.13}$$

and

$$\sin\theta = \sqrt{(1-z)/2}. \tag{2.14}$$

In order to have the few-body Integrodifferential equation operating over a valid fixed range, we make use of equation (2.9) to set the relative position vector for particle i and

j [3, 12, 16, 19]

$$\boldsymbol{r_{ij}} = rz = r\cos\phi_N^{ij} = r\sqrt{(1+z)/2} \tag{2.15}$$

or

$$\boldsymbol{r_{ij}} = rz = r\sin\phi_N^{ij} = r\sqrt{(1-z)/2}. \tag{2.16}$$

Using equations (2.13) and (2.14), we get

$$d\theta = \frac{dz}{2(1-z)^{1/2}(1+z)^{1/2}}. \tag{2.17}$$

Substituting equations (2.13), (2.14) and (2.17) in (2.10), then the surface element $d\Omega$ is written as [19]

$$d\Omega = \frac{1}{2^{\alpha+\beta+1}} W(z) dz d\omega d\Omega_{N-1}, \tag{2.18}$$

where $\Omega_{N-1} = (\omega_i, \theta_i, i = 1, ..., N-1)$. The weight function is given by

$$W(z) = (1-z)^{\alpha}(1+z)^{\beta}, \tag{2.19}$$

where parameters α and β are given by $\alpha = (D-5)/2$ and $\beta = 1/2$. To introduce the potential multipoles $V_K(r)$, where K represents the number of coupled equations to be solved, we first define the potential harmonics as [7, 19, 20]

$$\mathcal{P}^{L_m,m}_{2K+L_m}(\Omega_{ij}) = Y^m_{L_m}(\omega_{ij})^{(N)}\mathcal{P}^{L_m,m}_{2K+L_m}(\theta)\mathcal{Y}_{[0]}(D-3), \tag{2.20}$$

where $\mathcal{P}^{L_m,m}_{2K+L_m}(\Omega_{ij})$ is the potential harmonics of order $(2K+L_m)$, $Y^m_{L_m}(\omega_{ij})$ is the hyperspherical harmonics and $\mathcal{Y}_{[0]}(D-3)$ is the spherical harmonics of zero degree in $(D-3)$-dimensional space given by [7, 19, 21]

$$\mathcal{Y}_{[0]}(D-3) = \left[\frac{\Gamma(D-3)/2}{2\pi^{(D-3)/2}}\right]^{1/2}, \tag{2.21}$$

where Γ is the gamma function. In a many-body systems, particles move in an average central potential generated by all the particles [18]. To determine the hypercentral potential in S-state, we expand two-body potential $V^{\rho}(\boldsymbol{r_{ij}})$ in a complete set of potential harmonics as [7, 22, 23]

$$V^{\rho}(\boldsymbol{r_{ij}}) = \sum_{K=0}^{\infty} V_K^{\rho}(r)\mathcal{P}^{0,0}_{2K}(\Omega_{ij}), \tag{2.22}$$

where $\mathcal{P}^{0,0}_{2K}(\Omega_{ij})$ is the S-state potential harmonics derived from equation (2.20) and the superscript ρ represents a specific type of interacting pair of particles. The expansion coefficients $V^{\rho}_{K}(r)$ in equation (2.22) are called potential multipoles and are given by [7, 12, 17, 19]

$$\left.\begin{aligned} V^{\rho}_{K}(r) &= \mathcal{Y}_{[0]}(D-3)\int_{0}^{\pi/2} {}^{N}\mathcal{P}^{0,0}_{2K}(\theta)V(r\cos\theta)(\sin\theta)^{D-4}(\sin\theta)^{2}d\theta \\ &= \frac{1}{h^{\alpha,\beta}_{K}}\int_{-1}^{+1} V(\boldsymbol{r_{ij}})P^{\alpha,\beta}_{K}(z)W(z)dz. \end{aligned}\right\}, \tag{2.23}$$

where $h^{\alpha,\beta}_{K}$ is the normalization of equation (2.23) given by

$$h^{\alpha,\beta}_{K} = \int_{-1}^{+1}\left(P^{\alpha,\beta}_{K}(z)\right)^{2}W(z)\,dz. \tag{2.24}$$

2.2 Few-body Integrodifferential equation

The center of mass Schrödinger equation for many-body systems is defined as [12, 16, 17]

$$\left[-\frac{\hbar^{2}A}{M}\sum_{j=1}^{N}\nabla^{2}_{\boldsymbol{\zeta_j}} + \sum_{ij}^{A}V(\boldsymbol{r_{ij}})\right]\Psi(\boldsymbol{x}) = E\Psi(\boldsymbol{x}), \tag{2.25}$$

where A is the number of particles, position vector $\boldsymbol{r_i}$ (where $i = 1, ..., A.$), $V(\boldsymbol{r_{ij}})$ is the two-body potential operator for particles i and j, $\boldsymbol{r_{ij}} = \boldsymbol{r_i} - \boldsymbol{r_j}$, $\boldsymbol{x} \equiv \boldsymbol{r_1}, \boldsymbol{r_2}, ..., \boldsymbol{r_A}$ and E is the total energy of the system. In Faddeev formalism the many-body wave function is decomposed to construct the solution for Schrödinger equation for A-body systems in a form [12]

$$\Psi(\boldsymbol{x}) = \sum_{ij}^{A}\psi_{ij}(\boldsymbol{x}), \tag{2.26}$$

where $\psi_{ij}(\boldsymbol{x})$ are the Faddeev two-body amplitudes. The Faddeev two-body amplitudes depend on the degrees of freedom involved for all the particles in the system, satisfying $\frac{1}{2}A(A-1)$ coupled equations in the form

$$\left(\hat{T} + \sum_{i<j}^{A}V(\boldsymbol{r_{ij}}) - E\right)\sum_{i<j}\psi_{ij}(\boldsymbol{x}) = 0. \tag{2.27}$$

For a system with identical particles, the amplitudes $\psi_{ij}(\boldsymbol{x})$ can be written as follows [12, 17]

$$\psi_{ij}(\boldsymbol{x}) = H_{L_m}(\boldsymbol{x})F(\boldsymbol{r_{ij}}, r), \tag{2.28}$$

where $H_{L_m}(\boldsymbol{x})$ are harmonic polynomials of degree L_m and L_m standing for the quantum numbers which define the state of the system. Given that the center of mass in equation (2.6) is invariant under any exchange of particles, then the first term in the same equation is also invariant. The invariant behaviour of the kinetic energy operator for unequal particles in equation (2.6) enables us to generalize equation (2.28) so that we can derive the few-body Integrodifferential equation for unequal mass particles. Equation (2.28) is generalized as [12]

$$\psi^{\rho}_{ij}(\boldsymbol{x}) = H^{\rho}_{L_m}(\boldsymbol{x})F^{\rho}(\boldsymbol{\zeta}^{ij}_N, r), \tag{2.29}$$

where $\boldsymbol{\zeta^{ij}_N}$ is the vector $\boldsymbol{\zeta}_N$ of particles pair (ij). If quantum numbers $L_m = 0$, then [17]

$$H^{\rho}_{L_m}(\boldsymbol{x}) = H_0(\boldsymbol{x}) = constant. \tag{2.30}$$

Substituting equations (2.6) and (2.29) into equation (2.27) yields [6, 12, 17]

$$(T - E)F^{\rho}(\boldsymbol{\zeta^{ij}_N}, r) = -V^{\rho}(\boldsymbol{r_{ij}}) \sum_{i<j} F(\boldsymbol{\zeta^{ij}_N}, r). \tag{2.31}$$

The function $F(\boldsymbol{\zeta^{ij}_N}, r)$ can be determined by premultiplying equation (2.31) by $H_{[L_m]}(\boldsymbol{x})$ and then integrate over all variables except r and $\boldsymbol{\zeta^{ij}_N}$, setting

$$\left.\begin{aligned} z &= \cos 2\phi \\ &= \frac{2(\boldsymbol{\zeta^{ij}_N})^2}{r^2} - 1 \end{aligned}\right\}. \tag{2.32}$$

The relation of the radial coordinate $r \in [0, \infty]$ and the angular coordinate $z \in [-1, 1]$ of the few-body Integrodifferential equation is given by equations (2.15) and (2.16) [12, 19]. As a further simplification [12],

$$\left.\begin{aligned} G^{\rho}(z, r) &= r^{(D-1)/2} F^{\rho}\left(\boldsymbol{\zeta^{ij}_N}, r\right) \\ &= r^{(D-1)/2} G\left(\boldsymbol{r_{ij}}, r\right) \end{aligned}\right\}, \tag{2.33}$$

where $D = 3N$ and $N = A - 1$. As a consequence, the Faddeev two-body amplitudes $G(r, z)$ are the solution of the S-projected two-variable few-body Integrodifferential equation for identical particles given by [12, 16, 17, 19]

$$\left\{\frac{-\hbar^2}{m}\left[\frac{\partial^2}{\partial r^2}+\frac{1}{r^2}\left(4T_z-\frac{2L_m(L_m+1)}{1-z}-\frac{(3A-4)(3A-6)}{4}\right)\right]-E\right\}G^{\rho}(z,r) = -V^{\rho}(rz)\,\Theta^{\rho}(r,z), \tag{2.34}$$

where $L_m = (D-3)/2$ and

$$\Theta^{\rho}(r,z) = G^{(\rho)}(r,z) + \int_{-1}^{+1} f^{(\rho,\rho')}(z,z')G^{\rho'}(z',r)\,dz'. \tag{2.35}$$

The radial kinetic energy operator $\hat{T}_r$ is given by [12, 16]

$$\hat{T}_r = -\frac{\partial^2}{\partial r^2}, \tag{2.36}$$

for $L_m = 0$. The angular kinetic energy operator $\hat{T}_z$ of the system is given by [12, 17]

$$\hat{T}_z = \frac{1}{W(z)}\frac{\partial}{\partial z}(1-z^2)W(z)\frac{\partial}{\partial z}. \tag{2.37}$$

The projection of the amplitudes $F(\boldsymbol{\zeta}_N^{ij}, r)$ onto $\boldsymbol{\zeta}_N^{ij}$ give rise to the projection function $f^{\rho,\rho'}(z,z')$, which for identical particles eg. nucleon-nucleon or alpha-alpha interactions is given by [3, 12]

$$f^{\rho,\rho'}(z,z') = W(z')\sum_{K=1}^{\infty}\frac{f_K^2-1}{h_K^{\alpha,\beta}}P_K^{\alpha,\beta}(z)P_K^{\alpha,\beta}(z'), \tag{2.38}$$

where the constant [1, 12]

$$f_K^2 - 1 = \frac{A-2}{P_K^{\alpha,\beta}(1)}\left[2P_K^{\alpha,\beta}(-1/2)+\frac{1}{2}(A-3)P_K^{\alpha,\beta}(-1)\right] \tag{2.39}$$

and $P_K^{\alpha,\beta}$ are the Jacobi polynomials and the normalization $h_K^{\alpha,\beta}$ of the projection function is given by equation (2.23). Equation (2.34) can be modified by including the effects of higher partial waves by adding the zeroth ($K = 0$) order hypercentral potential multipole $V_0^{\rho}(r)$ generated using the potential multipole equation (2.23) on both sides of equation (2.31). The zeroth ($K = 0$) order hypercentral potential multipole is given by [24, 25]

$$V_0^{\rho}(r) = \frac{1}{h_0^{(\alpha,\beta)}}\int_{-1}^{+1} V(rz)W(z)dz. \tag{2.40}$$

This equation plays an important role in deriving the general few-body Integrodifferential equation for non-identical particles which is in the form [12]

$$\left\{\frac{-\hbar^2}{m}\left[\hat{H}+\sum_{\rho'}v_{\rho'}V_0^{\rho'}(r)\right]-E\right\}G^{\rho}(z,r)=-\left[V^{\rho}\left(r\sqrt{\frac{1+z}{2}}\right)-V_0^{\rho}(r)\right]\Theta^{\rho}(r,z), \tag{2.41}$$

where the kinetic energy operator when $L_m = 0$ is given by

$$\hat{H}=\frac{-\hbar^2}{m}\left[\frac{\partial^2}{\partial r^2}+\frac{1}{r_2}\left(4T_z-\frac{(3A-4)(3A-6)}{4}\right)\right], \tag{2.42}$$

$v_{\rho'}$ is the number of a given type ρ' and

$$\sum_{\rho'}v_{\rho'}=\frac{1}{2}A(A-1) \tag{2.43}$$

is the total number of pairs.

In this work, our solution is limited to identical particles, therefore superscripts on the two-body amplitudes and potentials are omitted since they are redundant. To this end, the few-body Integrodifferential equation (2.34) is cast into an eigenvalue problems in the form [12, 16, 17, 19, 24, 25]

$$\left[\hat{H}+V(rz)\right]G(r,z)+V(rz)\int_{-1}^{+1}f(z,z')G(r,z')\,dz'=EG(r,z). \tag{2.44}$$

It is worth noting that in the Fadeev-like equations, a spurious component of the potential which is not physical in nature is generated in the amplitudes $F(\boldsymbol{r_{ij}},r)$ by the hyperspherical harmonic

$$\mathcal{P}_{2K}^{0,0}(\Omega_{ij}) \tag{2.45}$$

present in the hyperspherical harmonics expansion of the potential $V(\boldsymbol{r_{ij}})$ in equation (2.22). Since

$$\sum_{i>j}\mathcal{P}_{2K}^{0,0}(\Omega_{ij})=0, \tag{2.46}$$

this component sum over all pairs in the Schrödinger equation. In order to eliminate the contribution of this spurious component, we subtract the first ($K = 1$) order potential

multipole

$$V_1(r) = \frac{1}{h_1^{(\alpha,\beta)}} \int_{-1}^{+1} V(rz) P_1^{\alpha,\beta}(z) W(z) dz, \tag{2.47}$$

where $P_1^{\alpha,\beta}(z)$ is the Jacobi polynomial of degree 1. To this end, we replace $V(rz)$ in equation (2.44) by [24, 25]

$$\bar{V}(rz) = V(rz) - V_1(r), \tag{2.48}$$

where $\bar{V}(rz)$ is the two-body nuclear potential with the spurious component of the potential eliminated. Substituting equation (2.48) into equation (2.44), the few-body Integrodifferential equation (2.44) is modified to [24, 25]

$$\left[\hat{H} + \bar{V}(rz)\right] G(r,z) + \bar{V}(rz) \int_{-1}^{+1} f(z,z') G(r,z')\, dz' = \bar{E} G(r,z), \tag{2.49}$$

where $\bar{E}$ are energies of the system obtained with the spurious component of the potential eliminated. The boundary conditions for bound-states solutions to satisfy two-body amplitudes $G(r,z)$ are determined first by physical properties of the system using quantum mechanics principles [14]. The type of interacting potentials are also essential in determining such boundary conditions. The asymptotic short and long-range radial forms of the two-body amplitudes are given by [27]

$$G(r,z) \xrightarrow{r\to 0} r^{(3A-4)/2} \tag{2.50}$$

and

$$G(r,z) \xrightarrow{r\to\infty} e^{-\sqrt{E_n} r} \tag{2.51}$$

respectively, where E_n is the energy of one of the states of the system. The asymptotic forms translates into boundary conditions [28]

$$G(0,z) = G(\infty,z) = 0, \tag{2.52}$$

which are important for eliminating the singularity of the kinetic energy matrix of the few-body Integrodifferential equation. The amplitudes are also expected to vanish at all singularities of the kinetic energy operator. Because the angular component of the kinetic

energy operator does not have singularities, therefore the boundary conditions

$$G(r, \pm 1) \neq 0, \tag{2.53}$$

are adopted. That is, if the potential does not have singularities in the z domain, $G(r, \pm 1)$ are functions of r.

In the next chapter, we outline the principles of the Lagrange-mesh method and construct a direct numerical solution to the few-body Integrodifferential equations (2.44) and (2.49), using the Lagrange-mesh method through the expansion of the Faddeev two-body amplitudes $G(r, z)$ on the Lagrange basis functions [14].

Chapter 3

Lagrange-mesh method

3.1 Principles of the Lagrange-mesh method

The Lagrange-mesh method is defined as a variational method that arises from the choice of basis involving orthogonal polynomials and the associated Gauss quadrature. We begin by defining a set of N Lagrange basis functions $f_i(x)$, valid over (a, b) which satisfy the condition [14]

$$f_i(x_j) = \lambda_i^{-1/2}\delta_{ij}, \tag{3.1}$$

where δ_{ij} is the Kronecker delta with x_i and λ_i as quadrature roots and weights respectively. According to the definition of the Lagrange-mesh method, each of the functions $f_i(x)$ vanish at all points except one. The Gauss quadrature approximation, which is a numerical integral approximation in the domain (a,b) is given by [14, 15]

$$\int_a^b g(x)dx \approx \sum_{i=1}^{N} \lambda_i g(x_i), \tag{3.2}$$

where $g(x)$ is a real function. Condition (3.1) of the Lagrange basis functions ensures that the basis functions are exactly orthonomal with the Gauss quadrature [15]

$$\int_a^b f_i^*(x)f_j(x)dx = \sum_{k=1}^{N} \lambda_k f_i(x_k)f_j(x_k) = \delta_{ij}. \tag{3.3}$$

Let us consider the one-dimensional Schrödinger equation

$$-\frac{d^2\psi(x)}{dx^2} + V(x)\psi(x) = E\psi(x), \tag{3.4}$$

where $\psi(x)$ is the wave function, $V(x)$ the potential energy and E the energy operator of the system. In this case, the kinetic energy operator of the system is given by

$$T = -\frac{d^2\psi(x)}{dx^2}. \tag{3.5}$$

The wave function $\psi(x)$ in equation (3.4) is expanded on the Lagrange basis functions $f_i(x)$ as [14]

$$\psi(x) = \sum_{j=1}^{N} C_j f_j(x). \tag{3.6}$$

The use of the property of Lagrange basis at points x_i, generates the linear variational coefficients C_i given by [14, 15, 29, 30]

$$C_i = \lambda_i^{1/2}\psi(x_i). \tag{3.7}$$

To solve one-dimensional Schrödinger equation, we multiply f_i by equation (3.4) and then integrate in the interval $(0, \infty]$ which can only be achieved with the help of the Lagrange-mesh property in equation (3.3) to yield [14]

$$\sum_{j=1}^{N} \left[T_{ij} + V_{ij}\right] C_j = EC_i. \tag{3.8}$$

When the Lagrange functions are generated from orthogonal polynomials, they create diagonal matrix elements for local potentials using the Gauss quadrature given by

$$V_{ij} \approx \int_a^b f_i^*(x)V(x)f_j(x)dx = \sum_{k=1}^{N} \lambda_k f_i(x_k)V(x_k)f_j(x_k) = V(x_i)\delta_{ij}, \tag{3.9}$$

for any potential function $V(x)$. In this basis, the matrix elements of the kinetic energy operator $-\dfrac{d}{dx^2}$, is evaluated as [14, 15]

$$T_{ij} \approx \int_a^b \lambda_k f_i(x_k)f_j''(x_k)dx = -\lambda_i^{1/2} f_j''(x_i), \tag{3.10}$$

where $f_j''(x_i)$ is the second derivative of the Lagrange basis functions. Substituting equations (3.7) and (3.9) in equation (3.8) yield [14, 15, 27]

$$\sum_{j=1}^{N} \left(T_{ij} + V(x_i)\delta_{ij}\right) \lambda_j^{1/2} \psi(x_j) = E\lambda_i^{1/2} \psi(x_i). \tag{3.11}$$

The Schrödinger equation presents a singularity at the origin of the coordinates of a Coulomb potential therefore functions $f_i(x)$ are not directly used because they do not behave appropriately around the origin. While the wave functions vanish around the origin, the Lagrange-Laguerre basis functions $f_i(x)$ do not vanish. Therefore, a non-linear scaling parameter h aimed at adjusting the mesh to finite domain of physical interest is introduced and the new regularized Lagrange-Laguerre functions are now defined by [15]

$$f_j(x) = h^{-1/2} f_j(x/h). \tag{3.12}$$

Equation (3.4) is cast into an eigenvalue problem for calculating the binding energies of one-dimensional Schrödinger equation in the form [14, 15, 27]

$$\sum_{j=1}^{N} \left[-h^{-2}\lambda_i^{1/2} f_j''(x_i) + V(hx_i)\delta_{ij}\right] C_j = EC_i \tag{3.13}$$

In the next section, we discuss the Lagrange-Laguerre $f_i(r)$ and Lagrange-Jacobi $g_j(z)$ as examples of Lagrange basis functions used to construct an eigenvalue problem.

3.2 Lagrange basis functions

The Lagrange-mesh method requires special basis of functions called the Lagrange basis functions. These functions are infinitely differentiable and vanish at mesh points but one which is associated with the mesh. That is to say, the Lagrange basis functions $f_i(r)$ and $g_j(z)$ vanish at all points except r_i and z_j respectively. One of the most important attributes of these functions is that they form an orthogonal set at the Gauss quadrature points [14, 30]. When the Lagrange basis functions are used in quantum mechanical

problems, they lead to simple algebraic expressions for the matrix elements of the Hamiltonian of the system [14]. A number of Lagrange basis functions exist [14]. In our study we choose, we choose Lagrange basis functions related to eigenfunctions of the Laplacian. These are the Lagrange-Laguerre and Lagrange-Jacobi basis functions. When the Hamiltonian of the system contains singularities, these Lagrange basis functions are regularized [14, 15].

3.2.1 Lagrange-Laguerre basis functions

The Lagrange-Laguerre basis functions are important in representing the radial component of the bound-state problem at a given mesh and are defined over an interval $(0, \infty)$. As it can be observed from Fig. 3.1, the regularized Lagrange-Laguerre functions are displayed for $\alpha = 1/2$ and $N_r = 5$ and they all vanish at $r = 0$ and their amplitudes increases as the distance r increases, for the chosen parameters α, β and N_r [14]. The regularization of the Lagrange-Laguerre functions by r is for practical application in bound state studies of the Schrödinger equation and to avoid inaccurate results for matrix elements at $1/r$ and $1/r^2$ [14]. The Lagrange-Laguerre basis functions are defined by [14]

$$f_i(r) = (-1)^i \left[\frac{r_i r^2 w^L(r)}{h^\sigma_{N_r}}\right]^{1/2} \frac{L^\sigma_{N_r}(r)}{r - r_i}, \tag{3.14}$$

where $w^L(r) = r^\sigma e^{-r}$ is the weight function of the Lagrange-Laguerre polynomials $L^\sigma_{N_r}$ of order N_r and $\sigma = 3A - 5$. The mesh points r_i are the roots of the Lagrange-Laguerre polynomials [14, 30]

$$L^\sigma_{N_r}(r_i) = 0, \tag{3.15}$$

where $i = 1, ..., N_r$. The Lagrange-Laguerre basis functions are normalized by [14]

$$h^\sigma_{N_r} = \frac{\Gamma(N_r + \alpha + 1)}{N_r!}. \tag{3.16}$$

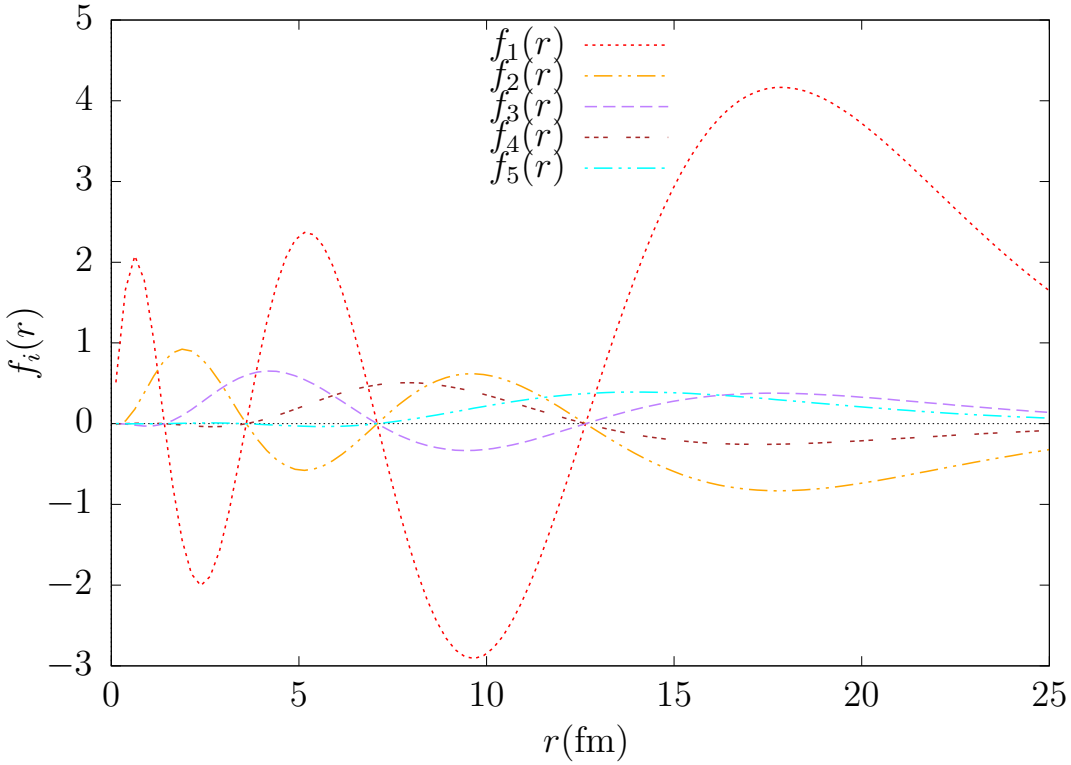

Figure 3.1: Regularized Lagrange-Laguerre functions with the number of radial points $N_r = 5$.

The radial kinetic energy operator is given by equation (2.36) and its matrix elements using the Gaussian approximation is given by [14]

$$\left.\begin{aligned} T^r_{ik} &= (-1)^{i-k}\frac{(r_i+r_k)}{\sqrt{r_i r_k}(r_i-r_k)^2}; \qquad i \neq k \\ &= \frac{4-\sigma^2}{12r_i^2} + \frac{2N_r+\sigma+1}{6r_i} - \frac{1}{12}; \qquad i = k \end{aligned}\right\}. \tag{3.17}$$

The radial kinetic energy matrix elements T^r_{ik} are also exact when treated with Gauss quadrature as their corresponding Lagrange-Laguerre basis functions [30].

3.2.2 Lagrange-Jacobi basis functions

The Lagrange-Jacobi basis functions in this case are used to approximate the Faddeev two-body amplitudes and used to construct the matrix element of the angular component of kinetic energy of the few-body Integrodifferential equation. The Jacobi polynomials $P^{\alpha,\beta}_{N_z}(z)$ are defined over the interval (-1,1), that can be observed by concentration of the mesh-points within this interval in Fig. 3.2. The Lagrange-Jacobi basis functions are defined by [14, 32]

$$g_j(z) = (-1)^{N_z-j}\left[\frac{(1-z^2)^\mu w^J(z)}{h^{\alpha,\beta}_{N_z}(2N_z+\gamma)(1-z_j^2)^{\mu-1}}\right]^{1/2}\frac{P^{\alpha,\beta}_{N_z}(z)}{z-z_j}, \tag{3.18}$$

where $w^J(z) = (1-z)^\alpha(1+z)^\beta$ is the weight function of the Lagrange-Jacobi polynomials $P^{\alpha,\beta}_{N_z}$ of order N_z, the regularization parameter $\mu = -1/2$ and parameter $\gamma = \alpha+\beta+1$. The mesh points z_j are the roots of the Lagrange-Jacobi polynomials [14, 32]

$$P^{\alpha,\beta}_{N_z}(z_j) = 0, \tag{3.19}$$

where $j = 1, ..., N_z$. The Lagrange-Jacobi basis functions are normalized by [14]

$$h^{\alpha,\beta}_{N_z} = \frac{2^\gamma}{2N_z+\gamma}\frac{\Gamma(N_z+\alpha+1)\Gamma(N_z+\beta+1)}{N_z!\Gamma(N_z+\gamma)}. \tag{3.20}$$

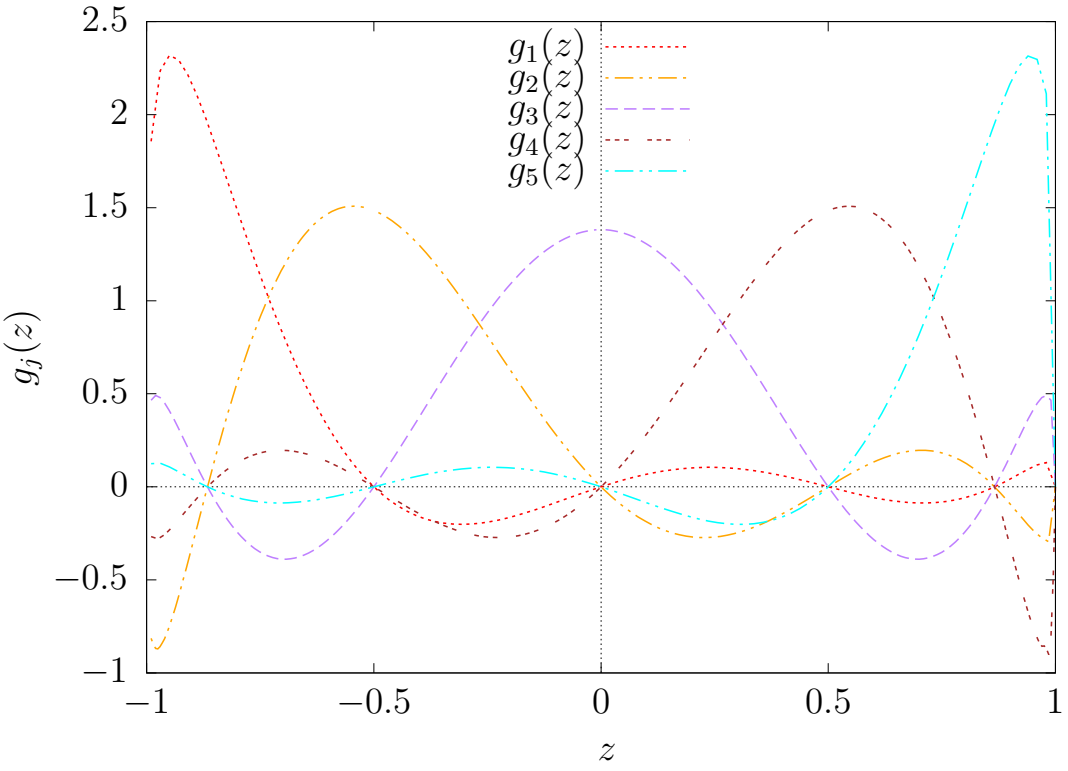

Figure 3.2: Regularized Lagrange-Jacobi functions with the number of radial points $N_z = 5$.

Similarly, to construct kinetic energy matrix elements of the angular component, the angular kinetic energy operator (2.37) is applied on the Lagrange-Jacobi basis functions (3.18) as

$$T^z_{jl} = \left\langle g_j(z)|(1-z^2)\frac{d^2}{dz^2} - z\frac{d}{dz}|g_l(z)\right\rangle . \tag{3.21}$$

The constructed angular kinetic energy matrix elements $T_{jl}(z)$ are in the form [32]

$$\left.\begin{aligned} T^z_{jl} &= (-1)\left(\frac{1-z_j^2}{1-z_l^2}\right)^{(\mu-1)/2}\left[\frac{u-\nu z_i}{z_j-z_j} - \frac{2(1-z_j^2)}{(z_j-z_l)^2}\right]; \qquad j\neq l \\ &= \frac{1-(2N_z+\gamma)^2}{12} + \frac{\omega_0+\omega_1 z_j+\omega_2 z_j^2}{6(1-z_j^2)}; \qquad j=l \end{aligned}\right\} . \tag{3.22}$$

The parameters are $u, \nu, \omega_0, \omega_1$ and ω_2 which are simple functions of β, α and μ are given by

$$\left.\begin{aligned} u &= \beta_0 - \alpha_0 \\ \nu &= \alpha_0 + \beta_0 + 2\mu \\ \omega_0 &= \alpha^2 + \beta^2 - 6\mu + 4 \\ \omega_1 &= \alpha^2 - \beta^2 - 6u(\mu-1) \\ \omega_2 &= 6(\nu-\mu)(\mu-1) \end{aligned}\right\} . \tag{3.23}$$

The parameters of the Lagrange-Jacobi basis functions were set to $(\alpha, \beta) = (\alpha_0, \beta_0)$ which correspond to the eigenfunctions of the angular kinetic energy operator. Therefore

$$W(z) = w^J(z) = (1-z)^{\alpha_0}(1+z)^{\beta_0}, \tag{3.24}$$

which implies that $\alpha_0 = (3A-8)/2$ and $\beta_0 = L_m + 1/2 = 1/2$ when $L_m = 0$. Similarly, the matrix elements T^z_{jl} are exact when treated with the Gauss quadrature as their corresponding basis Lagrange-Jacobi basis functions [32].

3.3 Construction of the matrix elements

To model the behaviour of various nuclei, one has to extract the unknown Faddeev two-body amplitudes $G(r, z)$ of the few-body Integrodifferential equation given in chapter 2 by equations (2.44) and (2.49). Since the exact expression of the two-body wave function is difficult to extract from the two-variable few-body Integrodifferential equation, we express the Faddeev two-body amplitudes $G(r, z)$ in terms of a linear combination of Lagrange basis functions $f_i(r)$ and $g_j(z)$ as [14]

$$G(z, r) = \sum_{i}^{N_r} \sum_{j}^{N_z} C_{ij} f_i(r) g_j(z), \tag{3.25}$$

where C_{ij} are linear variational coefficients and $f_i(r)$ and $g_j(z)$ are the real Lagrange-Laguerre 3.14 and Lagrange-Jacobi functions 3.18. The Lagrange functions are defined on the mesh points r_i (where $i = 1, 2, 3..., N_r$) and z_j (where $j = 1, 2, 3, ..., N_z$) which are the roots of the Lagrange-Laguerre and Lagrange-Jacobi respectively as mentioned in the previous section. The linear variational coefficients C_{ij} are expressed using the property of the Lagrange basis at points r_i and z_j in the form

$$C_{ij} = \sqrt{\lambda_i \lambda_j} G(r_i, z_j). \tag{3.26}$$

To construct an eigenvalue problem of the few-body Integrodifferential equations (2.44) and (2.49), we multiply equations (2.44) and (2.49) by $f_k(r) g_l(z)$ and then integrate over the problem domain with the help of Lagrange-mesh property given by equation (3.3), which describes the orthonomality of Lagrange functions with the Gauss quadrature to get [14, 30]

$$\sum_{kl} \left[H^0_{ij,kl} + V_{ij,kl} \right] C_{kl} = E C_{ij}, \tag{3.27}$$

where $H^0_{ij,kl}$ and $V_{ij,kl}$ are the kinetic energy matrix elements and potential energy matrix of the system respectively. The potential matrix elements are approximated using the

Gauss quadrature. Using equation (3.25) and (3.26), the potential energy term

$$V(rz)\left[G(r,z)+\int_{-1}^{+1} f^{\alpha,\alpha'}(z,z')G(r,z')\,dz'\right] \tag{3.28}$$

in few-body Integrodifferential equations (2.44) and (2.49) is evaluated using the Lagrange-mesh method to give [14]

$$V(r_i,z_l)\left[\delta_{jl}+\sqrt{\lambda_j\lambda_l}f(z_l,z_j)\right]\delta_{ik}. \tag{3.29}$$

The generated potential energy matrix elements of the system is given by

$$V_{ij,kl}=\left(V(r_i,z_l)\delta_{jl}+\sqrt{\lambda_j\lambda_l}V(r_i,z_l)f(z_l,z_j)\right)\delta_{ik}. \tag{3.30}$$

Parameters λ_j and λ_l are given by

$$\lambda_j = w_j^J/w(z_j) \tag{3.31}$$

and

$$\lambda_l = w_l^J/w(z_l), \tag{3.32}$$

where w_j^J and w_l^J are Gauss quadrature weights and $w^J(z_j)$ and $w^J(z_l)$ are Lagrange-Jacobi weight functions. The Lagrange-mesh kinetic energy matrix elements are evaluated as [14, 32]

$$H^0_{ij,kl}=\frac{\hbar^2}{m}\left[T^r_{ik}\delta_{jl}-\frac{1}{r_i^2}\left(4T^z_{jl}-\frac{\sigma^2-1}{4}\delta_{jl}\right)\delta_{ik}\right]. \tag{3.33}$$

The matrix elements T^r_{ik} and T^z_{jl} of the few-body Integrodifferential equations are those given by (3.17) and (3.22) respectively [14, 32]. The substitution of equations (3.30) and (3.33) in equation (3.27) yield

$$\sum_{kl}\left\{H^0_{ij,kl}+\left(V(r_i,z_l)\delta_{jl}+\sqrt{\lambda_j\lambda_l}V(r_i,z_l)f(z_l,z_j)\right)\delta_{ik}\right\}C_{kl}=EC_{ij}. \tag{3.34}$$

To avoid singularities of the few-body Integrodifferential equation at the origin, the Lagrange-Laguerre basis functions are adapted by scaling factor h, to modify the few-body Integrodifferential equation to the form [14, 15]

$$\sum_{kl}\left[\frac{1}{h^2}H^0_{ij,kl}+\left(V(hr_i,z_l)\delta_{jl}+\sqrt{\lambda_j\lambda_l}V(hr_i,z_l)f(z_l,z_j)\right)\delta_{ik}\right]C_{kl}=EC_{ij}. \tag{3.35}$$

Similarly, the modified few-body Integrodifferential equation (3.35) with the spurious potential $V_1(r)$ eliminated is solved directly using the Lagrange-mesh and takes a form

$$\sum_{kl}\left[\frac{1}{h^2}H^0_{ij,kl}+\left(\bar{V}(hr_i,z_l)\delta_{jl}+\sqrt{\lambda_j\lambda_l}\bar{V}(hr_i,z_l)f(z_l,z_j)\right)\delta_{ik}\right]C_{kl}=\bar{E}C_{ij}. \tag{3.36}$$

In the next chapter, we test the accuracy of the direct numerical solution to the few-body Integrodifferential equation by calculating and discussing ground-state binding energies for A-body systems interacting via selected two-body nuclear potentials.

Chapter 4

Results and Discussion

4.1 Parameter space

The numerical integration of the few-body Integrodifferential equations (3.35) and (3.36) involves many parameters such as μ, σ, h, r, N_r and N_z. In order to obtain accurate and converged binding energies, these parameters must be optimized. To numerically solve equations (3.35) and (3.36), we first truncated the hyperradius r by $r_{\max}$ and the angular coordinate z by $z_{\max} = 1$. Then the intervals $[0, r_{\max}]$ was discretized into N_r radial points equally spaced by parameter $h = r_{\max}/N_r$, while the interval $[z_{\min}, z_{\max}]$ was discretized into N_z points, also equally spaced. A Fortran code was developed to solve the matrix eigenvalue problem.

4.2 Two-body nuclear potentials

In this work, semi-realistic two-body nuclear potentials, such as the alpha-alpha Ali-Bodmer [33] and the nucleon-nucleon Volkov [34] as well as the MTV [35, 36], which are commonly used in benchmark calculations, are also adopted as inputs in our numerical calculations. This would enable us to compare our results with those in the literature of competing methods. Although these potentials are central potentials, they provide realistic description of nuclear systems. The treatment of spin dependent potentials in the current approach is straight forward [6, 37]. The parameters of these potentials were determined by fitting experimental scattering data.

4.2.1 Alpha-alpha potential

When many-body systems like ^{12}C and ^{16}O exhibit alpha clustering, one can resort to alpha-alpha potentials. To this end, we use the Ali-Bodmer which has a soft core and is given by [33]

$$V(r) = v_1 e^{-r^2 b_1^2} - v_2 e^{-r^2 b_2^2}, \tag{4.1}$$

where parameters v_1, v_2, b_1, and b_2 are listed in Table 4.1.

4.2.2 Nucleon-nucleon potentials

Two different nucleon-nucleon potentials are used in this work, namely the Volkov potential and the MTV potential. The Volkov potential is given by [34]

$$V(r) = -v_1 e^{-r^2/b_1^2} + v_2 e^{r^2/b_2^2}, \tag{4.2}$$

and on the other hand, the MTV potential is given by [35, 36]

$$V(r) = -\frac{v_1}{r} e^{-r b_1} + \frac{v_2}{r} e^{-r b_2}. \tag{4.3}$$

Equations (4.2) and (4.3) clearly indicate that the Volkov potential has a softer core as compared to MTV potential since $V(r) \xrightarrow{r \to 0} \infty$. Parameters v_1, v_2, b_1, and b_2 for these two-body nuclear potentials are also listed in Table 4.1.

Table 4.1: Parameters v_1, v_2, b_1 and b_2 for Volkov, Ali-Bodmer and MTV nuclear potentials employed in this work.

	Parameters			
Potential	v_1 (MeV)	v_2 (MeV)	b_1	b_2
Ali-Bodmer	500	130	0.7 fm^{-1}	0.475 fm^{-1}
Volkov	83.34	144.86	1.6 fm	0.82 fm
MTV	578.09	1458.05	1.55 fm^{-1}	3.11 fm^{-1}

Looking again at Fig. 4.1(a), it can be observed that the MTV potential has a slightly longer tail than both Ali-Bodmer and Volkov potentials. On the other hand it can be observed from the figure that the Ali-Bodmer is expected to give less binding energies because of weak attraction as r becomes smaller. It is further noticed in Fig. 4.1(a) that $V(r)$ fall rapidly to zero beyond $r = 15$ fm for all potentials and systems considered. Therefore, one would not expect any significant contribution of the ground-state binding energy beyond this value. In chapter 2, we have discussed the removal of the spurious component of the potential by subtracting the first order potential multipole $V_1(r)$. It is important to analyze how this component depends on the number of particles A. To this end, we plot in Fig. 4.1(b)-(d), the potential $V_1(r)$ as function of the hyperradius r for $A = 4, 5, 6, 7$, and for all the three potentials. Looking at Fig. 4.1(b), it is seen that $V_1(r)$ is exclusively repulsive. The potential is expected to generate the lowest binding energies as compared to the other potentials. It can be noticed that the repulsiveness increases with number of particles. As for Fig. 4.1(c), which corresponds to the $V(r)$ for the Volkov potential, we first notice that unlike in Fig. 4.1(a), $V_1(r)$ is fairly extended beyond $r = 15$ fm and this extension increases with the number of particles A. This shows that the numerical integration range will increase with A, as one would expect. In Fig. 4.1(d), one draws similar conclusions as in Fig. 4.1(c).

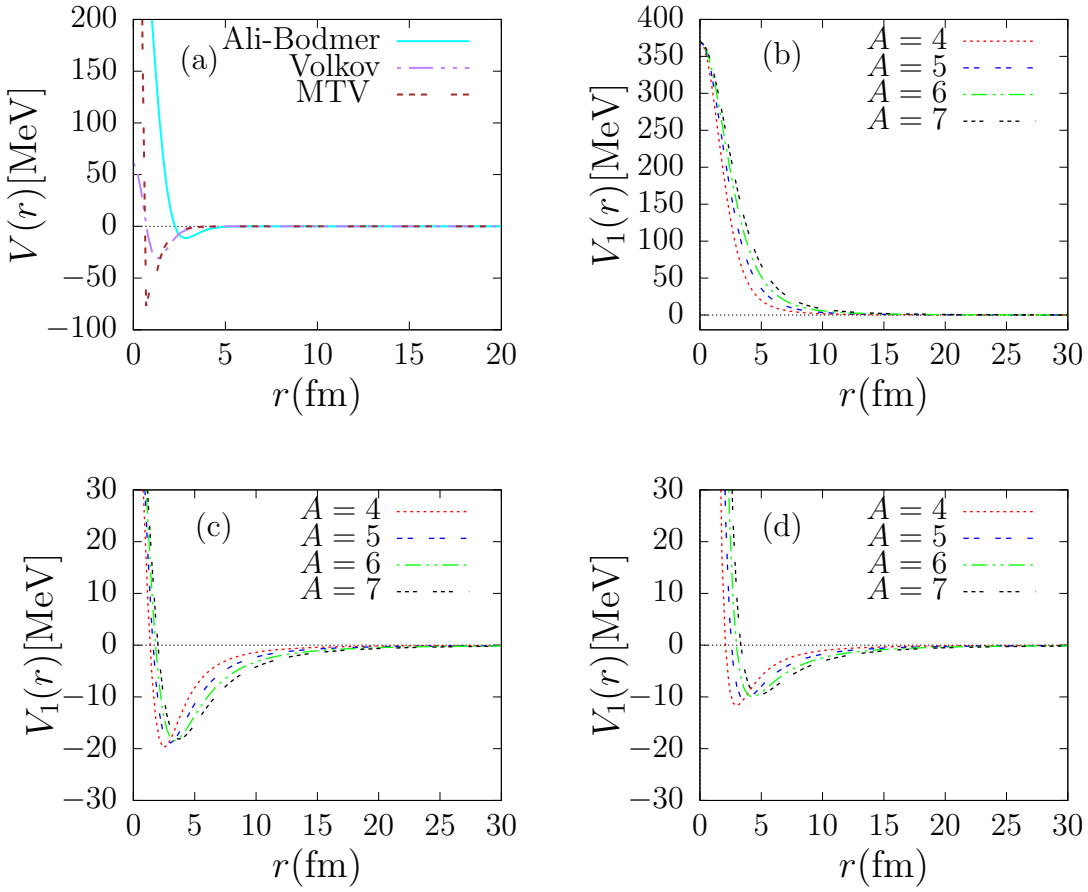

Figure 4.1: Plots for (a) two-body potentials for $A = 4$ as well as the corresponding (b)-(d) first ($K = 1$) order potential multipole $V_1(r)$ for the three potentials as a function of the hyperradius r for $A = 4, 5, 6, 7$.

4.3 Results for the Ali-Bodmer potential

In this section, we present and discuss the ground-state binding energies E obtained for A alpha cluster systems, using the soft core Ali-Bodmer potential as input. We calculate ground-state energies for $4\alpha, 5\alpha, 6\alpha$ and 7α systems with increasing number of radial points N_r. To obtain converged binding energies, the few-body Integrodifferential equation (3.35) was integrated to $r_{\max} = 30\,\text{fm}$, we used $N_z = 5$ for four-α system, $N_z = 6$ for five-α system and $N_r = 8$ for both six- and seven-α systems. For alpha cluster systems, the constant $\hbar^2/m = 10.367$ MeV.fm^{-2}. The obtained results are given in Table 4.2, where the convergence is checked against N_r for four-, five-, six- and seven-α systems.

As it can be seen from Table 4.2, the ground-state binding energies for all four systems considered indicates that excellent convergence is indeed achieved as N_r increases. It can be further noticed that the smaller A is, the faster the convergence. Our ground-state binding energies converge with increasing number of radial points to -11.289064, -17.635918, -20.284793 and -29.857322 MeV for four-, five-, six- and seven-α systems in the order mentioned. These results are in excellent agreement with those reported in literature. In particular with those obtained with the Stochastic variational method, where the differences (in percentage) with our results are 1.7%, 8% and 0.7% for four-, five- and six-α systems in the order mentioned [38].

To further highlight the convergence in Table 4.2, we plot in Fig. 4.2(a)-(d), the ground-state binding energies as a function of the radial basis size N_r. As it can be observed from this figure, as already noticed in Table 4.2, the ground-state binding energies converge rapidly at $N_r = 40$ for four- and five-α systems and $N_r = 50$ for six- and seven-α systems.

Table 4.2: Convergence of energies E in MeV for alpha cluster systems with the Ali-Bodmer potential as a function of number of radial points N_r when $r_{\max} = 30\,\text{fm}$.

	E (MeV)			
N_r	A=4	A=5	A=6	A=7
10	-12.803958	-18.342474	-21.408161	-30.993612
20	-11.263968	-17.671214	-20.048973	-30.331416
30	-11.289057	-17.636153	-20.279985	-29.888380
40	-11.289064	-17.635918	-20.284778	-29.857493
50	-11.289064	-17.635918	-20.284793	-29.857321
60	-11.289064	-17.635918	-20.284793	-29.857322
70	-11.289064	-17.635918	-20.284793	-29.857322
	Others			
	-11.07[38]	-16.22[38]	-20.13[38]	-
	-11.1[11]	-	-	-

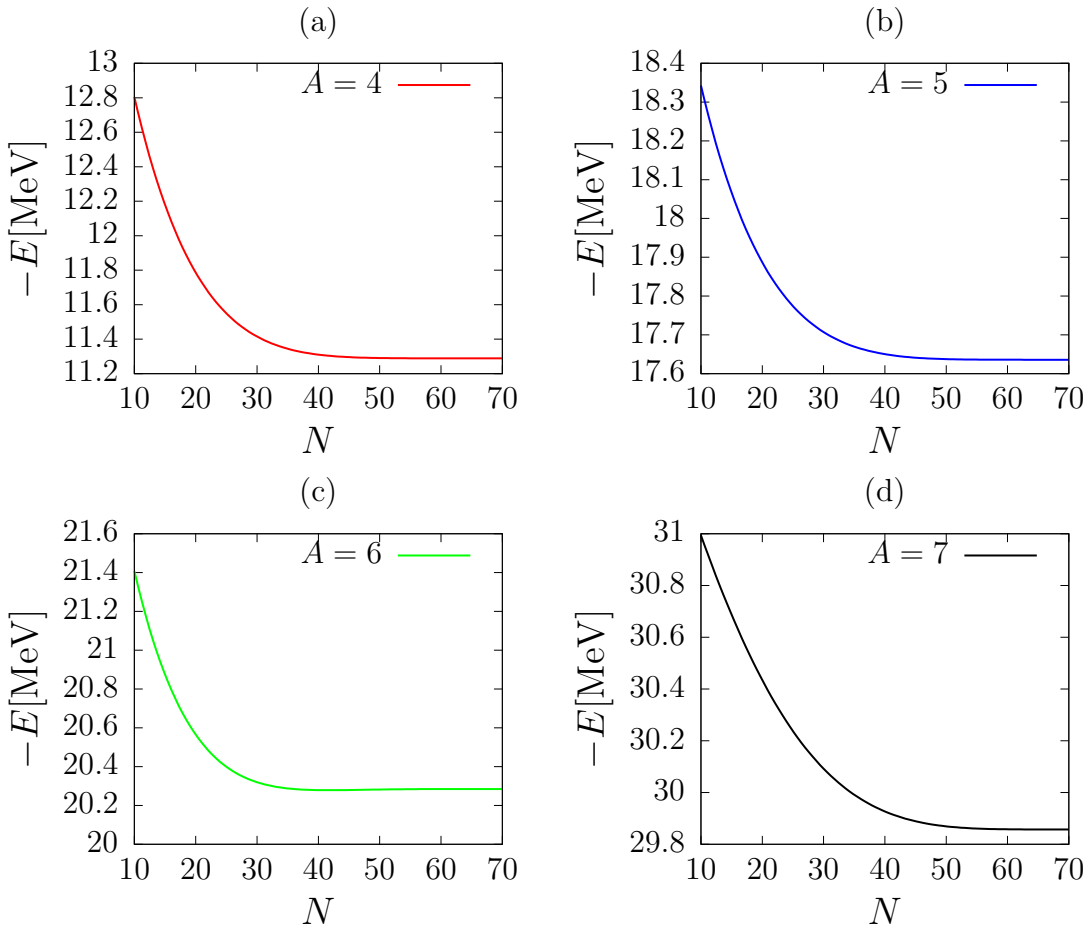

Figure 4.2: Plots of binding energies in MeV as a function of number of radial points N_r for alpha cluster systems interacting via the Ali-Bodmer potential.

The conclusion here, is that the Lagrange-mesh ground-state binding energies calculated are in perfect agreement with the Stochastic variational method for $A = 4, 5, 6$ with the Ali-Bodmer potential.

4.4 Results for the Volkov potential

The results in section 4.3, for alpha cluster systems have revealed a rather encouraging agreement with the consulted literature. To further test our approach, we now consider the case of A-body systems interacting via the nucleon-nucleon Volkov potential. As previously, we calculate the ground-state binding energies E. Only the convergence of the binding energies as function of the parameter N_r is shown in Table 4.3 and Fig. 4.3(a)-(d), where $r_{\max} = 30$ fm and $N_z = 6$. For nucleon-nucleon systems, the constant $\hbar^2/m = 41.467$ MeV.fm^{-2}. Again the same number of masses are considered, namely $A = 4, 5, 6, 7$.

Looking at Table 4.3 and Fig. 4.3(a)-(d), one notices a rapid convergence for all four systems considered. A good convergence is already obtained when the number of radial points $N_r = 30$ for all systems. The calculated ground-state energies converge to -29.515835, -66.397947, -119.888548, -190.291015 MeV for four-, five-, six- and seven-body systems in the order given.

Our energies once again are in perfect agreement with those obtained using the Hyperspherical harmonics expansion [10] and Perturbation [1] methods, where the differences (in percentage) with our results are 2.4%, 2.8%, 2.4% and 5% for four-, five-, six- and seven-body systems respectively [10, 1]. Our results are also compared to the ones obtained using the Stochastic variational method [38].

Table 4.3: Convergence of energies E in MeV for A-body nucleon-nucleon systems with the Volkov potential as a function of number of radial points N_r when $r_{\max} = 30\,\text{fm}$.

	E (MeV)			
N_r	A=4	A=5	A=6	A=7
10	-30.089133	-68.955840	-120.928968	-192.292780
20	-29.515797	-66.398077	-119.886847	-190.304828
30	-29.515835	-66.397947	-119.888548	-190.291015
40	-29.515835	-66.397947	-119.888548	-190.291015
50	-29.515835	-66.397947	-119.888548	-190.291015
60	-29.515835	-66.397947	-119.888548	-190.291015
70	-29.515835	-66.397947	-119.888548	-190.291015
	Others			
	-30.25[10]	-68.28[10]	-122.78[10]	-200.1364[1]
	-30.42[38]	-43.00[38]	-66.25[38]	-98.75[38]
	-30.27[11]	-	-	-

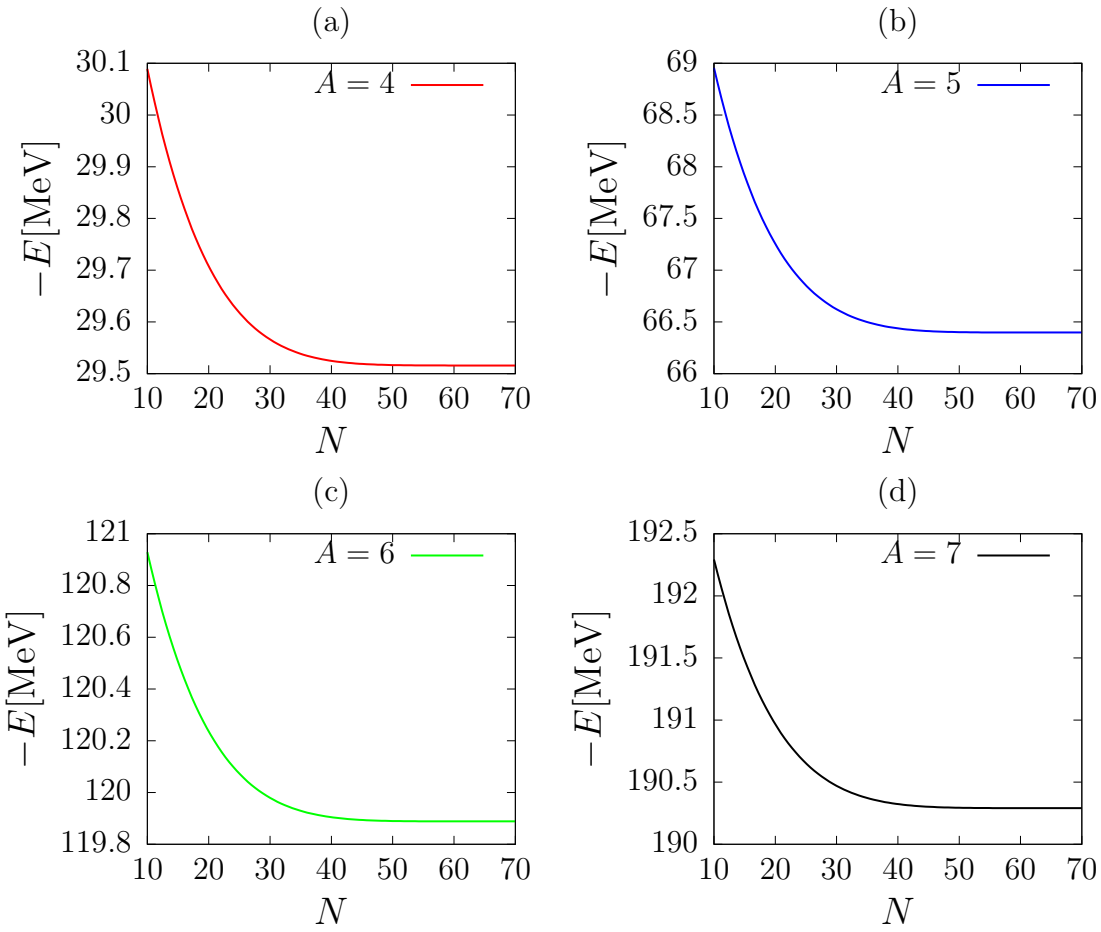

Figure 4.3: Plots of binding energies in MeV as a function of number of radial points N_r for A-body systems interacting via the Volkov potential.

It follows that the direct integration of the few-body Integrodifferential equation using Lagrange-mesh with the Volkov potential is in perfect agreement with other approximative methods, such as Hyperspherical harmonics expansion, Perturbation and Stochastic variational methods. In addition, the convergence here is faster than in the Ali-Bodmer case.

4.5 Results for the MTV

The results presented so far concern soft core potentials, it is important to also check the stability of our approach on a hard core potential. To this end, we consider in this section the MTV potential. The methodology remains similar to the two previous cases. That is, we considered the same systems and the convergence is carefully checked against the different integration parameters. A good convergence was guaranteed with $r_{\max} = 30$ fm, as previously with $N_Z = 9$. The results are summarized in Table 4.4(a)-(d).

Again convergence of the binding energies E as function of the number of radial points N_r is shown in the table. A careful look at this table shows that a good convergence is already reached at $N_r = 30$, for all four systems considered. Comparing with those available in literature, it is noticed that for the four-body system, our results are in good agreement. However, as A increases, we observe that our results disagree with literature results. Among others, one can argue that this is due to hard core nature of the MTV potential, particles cannot be too close to each other, thereby making the approximation of the integral inaccurate for higher partial waves as the number of particles increases [25].

As a result the ground-state binding energies for five-, six- and seven-body systems were poorly calculated and converged to large values resulting in large percentage differences as compared to those reported in [2, 19, 38] for six-body systems. The difference (in percentage) of our results to those in [17, 2] are 2.8% and 16% for four- and six-body systems in the order given. We further highlight the convergence of our results in Table 4.4 by plotting in Fig. 4.4(a)-(d), the ground-state binding energies as a function of the radial basis size N_r for four-, five-, six, and seven-body systems. As it can be observed from this figure, as already observed in Table 4.4, the ground-state binding energies converge rapidly to an exact value at $N_r = 40$ for four-body system and incorrect values for five-, six- and seven-body systems.

Table 4.4: Convergence of energies E in MeV for A-body nucleon-nucleon systems with the MTV potential as a function of number of radial points N_r when $r_{\max} = 30\,\text{fm}$.

	E (MeV)			
N_r	A=4	A=5	A=6	A=7
10	-31.822202	-73.032303	-136.745756	-231.857953
20	-31.522643	-74.434845	-140.524333	-228.474694
30	-31.522606	-73.434726	-138.523922	-228.487413
40	-31.522606	-73.434726	-138.523922	-228.487413
50	-31.522606	-73.434726	-138.523922	-228.487413
60	-31.522606	-73.434726	-138.523922	-228.487413
70	-31.522606	-73.434726	-138.523922	-228.487413
	Others			
	-31.36[38]	-43. 48[38]	-66.30[38]	-83.4[38]
	-30.63[17]	-	-116.41[2]	-
	-29.82[19]	-	-116.84[19]	-

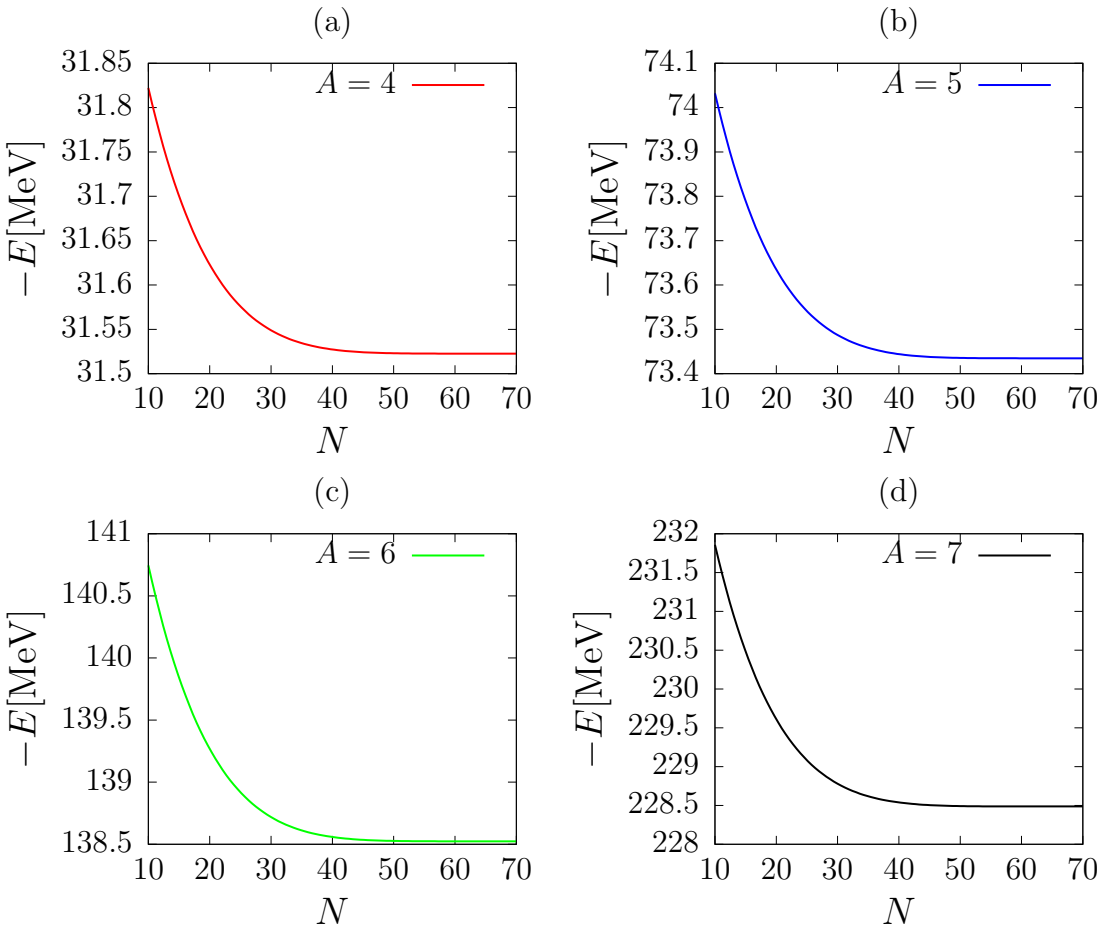

Figure 4.4: Plots of binding energies in MeV as a function of number of radial points N_r for A-body systems interacting via the MTV potential.

To further check the stability of our results, we also investigate the effect of spurious component of the potential on our results by calculating the ground-state binding energies $\bar{E}$ obtained with the spurious potential $V_1(r)$ removed in the next section. The calculations of ground-state binding energies $\bar{E}$ are obtained with increasing radial coordinate r. As it was observed, our results for nucleon-nucleon systems interacting via the MTV potential converged to values which are higher than those reported in literature with large percentage errors for five-, six- and seven-body systems. As a result, the effect of the spurious potential $V_1(r)$ was not investigated for this potential.

4.6 Effect of spurious component of the potential

The results so far discussed contain the contribution of spurious component $V_1(r)$ of the potential associated with Faddeev-type equations. It is not clear how significantly the spurious potential affects our calculated ground-state binding energies E. To this end, we investigate this effect by eliminating the spurious component by numerically solving the few-body Integrodifferential equation (3.36) which is obtained after replacing the $V(r)$ potential by $\bar{V}(r)$ as explicitly explained in chapter 2 and 3. We have verified that the integration parameters used in section 4.3 and 4.4 are still applicable for results obtained in this case.

However, before considering the details, let us first look at the potential $\bar{V}(r)$ as plotted in Fig.4.5. Looking at this figure, one notices that the soft core observed in Fig. 4.1 (a) and (b) has been eliminated. To check how this affects the results so far obtained, we present the ground-state binding energies $\bar{E}$ in Table 4.5 for alpha cluster $A = 4, 5, 6, 7$ systems interacting via the Ali-Bodmer and Table 4.6 for the Volkov potential.

The obtained results are further highlighted in Fig. 4.6 for alpha-alpha potential and in Fig. 4.6 for the Volkov potential. However, for completeness, the convergence is checked against the radial coordinate r. It is observed in these tables and figures, that a satisfactory convergence is obtained with $r = 30$ fm, especially for alpha-alpha potential. This amounts to saying that the spurious component of the potential has an insignificant effect on convergence and accuracy of the ground-state energies E.

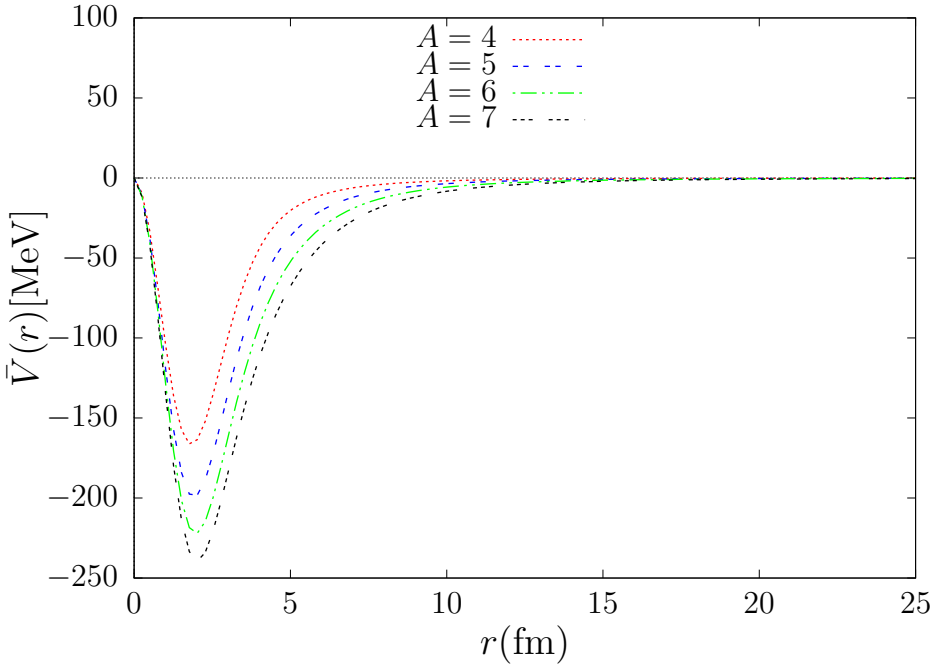

Figure 4.5: Plots of $\bar{V}(r)$ as a function of the hyperradius r for alpha-alpha particles interacting via the Ali-Bodmer potential for $A = 4, 5, 6, 7$.

Table 4.5: Variation of ground-state energies $\bar{E}$ in MeV as a function of the hyperradius r in fm for A-body alpha cluster systems interacting via the Ali-Bodmer potential.

	$\bar{E}$ (MeV)			
r (fm)	A=4	A=5	A=6	A=7
10	-5.287209	-7.911272	-7.331287	-4.189787
15	-11.176791	-14.013541	-12.545276	-14.084618
20	-11.289413	-17.635856	-18.589655	-25.568109
25	-11.289736	-17.637305	-20.285015	-29.857541
30	-11.289628	-17.638460	-20.286109	-29.859173
35	-11.289092	-17.638573	-20.287599	-29.861760
40	-11.288369	-17.637370	-20.288742	-29.864225
45	-11.287609	-17.635336	-20.288810	-29.865127
50	-11.286825	-17.633018	-20.287659	-29.863856

Table 4.6: Variation of ground-state energies $\bar{E}$ in MeV as a function of the hyperradius r in fm for A-body nucleon-nucleon systems interacting via the Volkov potential.

	$\bar{E}$ (MeV)			
r(fm)	A=4	A=5	A=6	A=7
5	-21.143435	-55.812475	-104.209978	-165.388565
10	-29.509552	-66.422591	-119.931003	-190.341746
15	-29.542475	-66.489720	-120.050257	-190.504862
20	-29.575618	-66.600379	-120.241006	-190.755612
25	-29.629009	-66.778155	-120.543407	-191.143513
30	-29.707616	-67.041085	-120.992410	-191.720462
35	-29.815274	-67.401871	-121.610302	-192.517342
40	-29.9550418	-67.870343	-122.413323	-193.554477
45	-30.129296	-68.454025	-123.413863	-194.847190
50	-30.339685	-69.157787	-124.619827	-196.405545

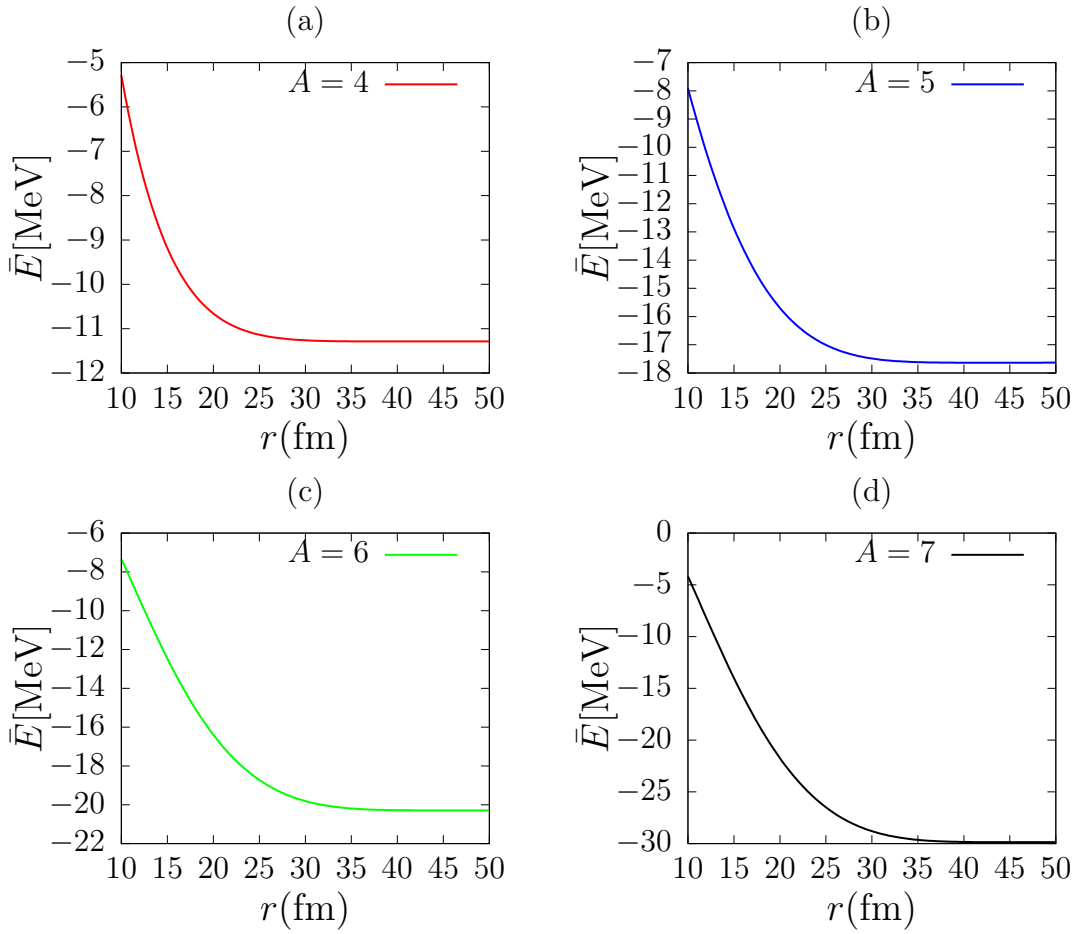

Figure 4.6: Plots of ground-state energies in MeV as a function r for A-body alpha-alpha systems interacting via the Ali-Bodmer potential.

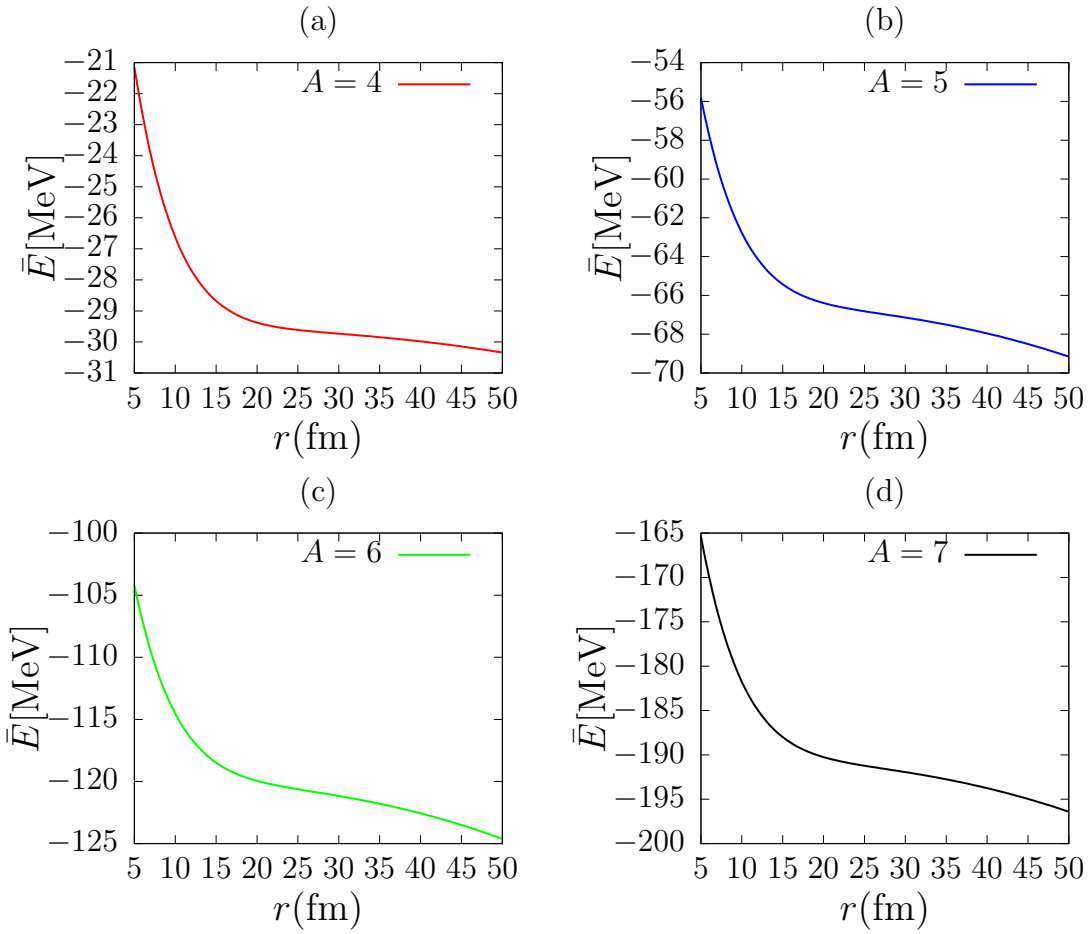

Figure 4.7: Plots of ground-state energies in MeV as a function of hypperradius r for A-body nucleon-nucleon systems interacting via the Volkov potential.

To better describe the effect of the spurious component, we present in Table 4.8 and Table 4.7, the differences ΔE between the binding energies obtained when this component is included and omitted in our calculations for the Ali-Bodmer and Volkov potentials. We only consider results for $r = 30$ fm, which is the value used to calculate the binding energies when the spurious component is included. As we can see from the tables, the effect of the spurious component is indeed small, especially for lighter systems. On the other hand, it is more important in alpha-alpha systems than in nucleon-nucleon systems.

Table 4.7: ΔE in MeV for alpha cluster systems interacting via the Ali-Bodmer potential when the number of radial points $N_r = 70$ and the hyperradius $r = 30$ fm.

	Number of particles (A)			
	4	5	6	7
ΔE (MeV)	0.000564	0.002542	0.001316	0.001851

Table 4.8: ΔE in MeV for A-body nucleon-nucleon systems interacting via the Volkov potential when the number of radial points $N_r = 70$ and the hyperradius $r = 30$ fm.

	Number of particles (A)			
	4	5	6	7
ΔE (MeV)	0.191781	0.643138	1.103862	3.730855

Chapter 5

Concluding Remarks

In this work, we have directly solved the few-body Integrodifferential equation using the Lagrange-mesh method. We first presented the mathematical derivation of the few-body Integrodifferential equation, starting from the expansion of the many-body wave function on the two-body Faddeev-type amplitudes. These amplitudes were in turn expanded on the Lagrange basis functions in order to obtain an eigenvalue problem, which was further solved numerically. To test the accuracy and stability of our method, we calculated the ground-state binding energies of A-body systems, where $A = 4, 5, 6, 7$ were calculated. The convergence of the results was checked against the numerical integration parameter N_r, while the other parameters were kept constant, subject to convergence requirements. A rapid convergence of the results is obtained for $N_r = 30$ with nucleon-nucleon potentials and $N_r = 40$ with the alpha-alpha Ali-Bodmer potential for all systems considered. The binding energies thus calculated were found to be in good agreement with those available in the literature, using different methods, especially for Volkov and Ali-Bodmer potentials. This indicates that, this method is as accurate as other competing methods with an added advantage of simplicity

In particular, with the Volkov potential, our results are in agreement with those available in the literature, with a general discrepancy of about 5% for $A = 4, 5, 6, 7$. On the other hand, the energies obtained with the alpha cluster Ali-Bodmer potential are in good agreement with those reported in the literature, with a general discrepancy of about 8% for $A = 4, 5, 6$. However, for the MTV potential, which exhibits a hard core and singularities at the boundary conditions, a considerable disagreement between our results

and those reported in the literature, was noticed for $A>4$. We also investigated the effect of the spurious component of the potential. To this end, we calculated the ground-state energies with the spurious component of the potential removed. Comparing the results obtained in the presence and absence of the spurious component, it is shown that the difference between the two binding energy is generally insignificant for the different systems considered. It would be interesting to investigate this effect for $A > 7$. The results obtained in this work, indicate that the Lagrange-mesh method is a promising tool for a direct solution to the few-body Integrodifferential equation.

Bibliography

[1] T. K. Das and R. Chattopadhyay : Fizika **B 2**, 262-502 (1993).

[2] N. Barnea and M. Viviani : Phys. Rev. **C 61**(3), 034003 (2000).

[3] R. M. Adam and S. A. Sofianos : Phys. Rev. **82**, 053635.1 (2010).

[4] L. D. Faddeev : Sov. Phys JETP. **12**, Davey, N.Y., 1014.1 (1961)

[5] S. A. Sofianos, G. J. Rampho, and R. M. Adam : Phys. Part. Nucl. **40**, 757.1 (2009).

[6] M. Fabre de la Ripelle : Few-Body Syst. **1** , 181-192 (1986).

[7] M. F. de la Ripelle : Ann. Phys. **147**, 281-320 (1983).

[8] F. Zernike and H. C. Brinkman : Proc. K. Ned. Akad. Wett. **38**, 161.1 (1935).

[9] M. Fabre de la Ripelle, M. Braun and S. A. Sofianos : Prog of Theo Phys. **98**(6), (1997).

[10] M. Gattobigio , A. Kievsky and M. Viviani : Phys. Rev. **C 83**(2), 024001.1 (2011).

[11] O. A. Yakubovskii : Sov. J. Nucl. Phys. **5**, 937.1 (1967).

[12] R.M. Adam and H. Fiedeldey : J. Phys. G: Nucl. Part. Phys. **19**, 701-719 (1993).

[13] S. Sanyal : Few-Body Syst **4**, 141-149 (1988).

[14] D. Baye : Physics Report **565**, 1-107 (2015).

[15] D. Baye : Atom. Mol. Opt. Phys. **28**, 4399.1 (1995).

[16] M. F. de la Ripelle , H Fiedeldey and S. A. Sofianos : Phys. Rev. **C 38**, 449-466 (1988).

[17] R .M. Adam, S. A. Safianos, H. Fiedeldey and M. Fabre de la Ripelle : J. Phys. G **18**, 1365-1375 (1992).

[18] M. F. de la Ripelle and J. Navarro : Ann. Phys. **123**, 285-232 (1979).

[19] B. Mukeru : MSc Dissertation. University of South Africa, (2006).

[20] B. Chakrabarti, A. Kundu, and T. K. Das : J. Phys. At. Mol. Opt. Phys **B8**, 2457-2466 (2005).

[21] J. S. Avery : J.Mat.Ch. **24**, 169-174 (1998).

[22] M. Fabre de la Ripelle, M. I. Haftel, and S. Y. Larsen : Phys. Let. **44**, 7084-7091 (1991).

[23] M. Fabre de la Ripelle, H. Fiedeldey and S. A. Sofianos : Few-body Syst. **6**, 157-174 (1989).

[24] R. Brizzi, M. Fabre De La Ripelle and M. Lassaut : Phys. **A 596**, 199-233 (1996).

[25] M. F. de la Ripelle and Y. S. Larsen : Few-Body Syst. **13**, 199-206 (1992).

[26] A. Bachkhaznadji and M. Lassaut : Few-Body Syst. **53**, (56) 1-7 (2014).

[27] D. Baye : J. Phys. B physica status solidi (b) **243**, 1095-1109 (2006).

[28] M. Vincke, L. Malegat and D. Baye : J. Phys. B: Atom. Mol. Opt. Phys. **26**, 1720.1 (1993).

[29] H. Masui, S. Aoyama 2 and D. Baye : Prog. Theor. Exp. Phys. **A02**, 123.1 (2013).

[30] M. Theeten : Phd thesis. university of Bruxelles (2009).

[31] G. J.Rampho : J. Phys. **CS 49** , 27501.1 (2016).

[32] G. J. Rampho : J. Phys. A: Math. Theor. **49**, 295202.1 (2016).

[33] S. Ali and A. Bodmer : Nucl. Phys, **80**, 99-112 (1966).

[34] A. Volkov : Nucl. Phys. **C 74**, 33-58 (1965).

[35] R. E. Malfiet and J. A. Tjon : Nucl. Phys. **A 127**, 161.1 (1969).

[36] G. J. Zabolitzky, K. E. Schmidt and M. H. Kalos : Phys. Rev. **C 25** , 1111.1 (1982).

[37] W. Oehm, S. A. Sofianos, H. Fiedeldey and M. F. de la Ripelle : Phys. Rev. **C 42**, 2322.1 (1990).

[38] K. Varga and Y. Suzuki : Phys. Rev. **C 52**, 2885.1 (1995).

[39] S. P. Merkuriev, S. L. Yakovlev, and C. Gignoux : Nucl. Phys. **A 431**, 125-138 (1984).

[40] G. J. Ramapho, L. C. Mabunda and M. Ramantswana : journal of physics:conf series **915**, 012005.1 (2017).

[41] H. Masui, S. Aoyama, and D. Baye : Prog. Theor. Exp. Phys. **A 02**, 123.1 (2013).

[42] D. Baye, M. Hesse and M. Vincke : Phys. Rev. **E 49**, 026701.

[43] Z. Papp and W. Plessas : Phys. Rev. **C 54**(1), 1476.1 (1996).

[44] K. Tapan Das and S. Roy : Pramana - J. Phys. **36**(3), 305-312 (1991).

[45] A. Kievsky, S. Rosati, M. Viviani, L. E. Marcucci and L. Girlanda : J. Phys. G: Nucl. Part. Phys. : **35**, 063101.1 (2008).

[46] T. K. Das T. K. and S. Roy : Pramana- J. Phys **36**, (1991).

[47] M. Fabre de la Ripelle : Phys. Letters. **B 753**, 8-12 (2016).

[48] J. L. Friar , B. F. Gibson and G. L. Payne : Phys. Rev. **C 24**, 227989.1 (1981).

[49] S. Flgge : Practical Quantum Mechanics (Berlin: Springer)(1999).

[50] P. Descouvemont ,C. Daniel and D. Baye : Phys. Rev. **C 67**, 044309.1 (2003).

[51] S. A. Sofianos and S. A. Rakityansky : J. Phys. **A 31**, 5149 (1998).

[52] H. Feldmeier : Nucl. Phys. **A 515**, 147 (1990).

[53] A. Ono, H. Horiuchi, T. Maruyama and A. Ohnishi : Prog. Theor. Phys. **87**, 1185 (1992).

[54] E. I. Tanaka, A. Ono, H. Horiuchi, T. Maruyama and A. Engel : Phys. Rev. **C 52**, 316.1 (1995).

[55] A. Engel, E. I. Tanaka, T. Maruyama, A. Ono and H. Horiuchi : Phys. Rev. **C 52**, 3231.1 (1995).

[56] R. D. Mattuck : A guide to Feymann diagrams in the Many-Body Problem. New York, second edition, (1967).

[57] A. Doté and H. Horiuchi : Prog. Theor. Phys. **103**, 261.1 (2000).

[58] A. Doté, Y. Kanada-En'yo, H. Horiuchi, Y. Akaishi and K. Ikeda : Prog. Theor. Phys. **115**, 1069.1 (2006).

[59] M. Kimura : Phys. Rev. **C 69**, 044319.1 (2004).

[60] A. Doté, H. Horiuchi, and Y. Kanada-En'yo : Phys. Rev. **C 56**, 1844.1 (1997).

[61] T. Togashi, K. Kat$\bar{o}$: Prog. Theor. Phys. **117**, 189.1 (2007).

[62] T. Togashi, T. Murakami and K. Kat$\bar{o}$: Prog. Theor. Phys. **121**, 29.19 (2009).

[63] T. Watanabe and S. Oryu : Prog. Theor. Phys. **116**, 429 (2006).

[64] T. Watanabe, M. Oosawa, K. Saito and S. Oryu : J. Phys. G : Nucl. Part. Phys. **36**, 015001.1 (2009).

[65] D. Brink : Proceedings of the International School of Physics "Enroco Fermi," Course 36, Edited by C. Bloch, (Academic, New York, 1965).

[66] D. W. Jepsen and J. O. Hirschfelder : Proc. Natl. Acad. Sci. U.S.A. **45**, 249.1 (1959).

[67] M.R. Hadizadeh A. and Khaledi-Nasab : Nucl. Phys. **A 752**, 321c (2005).

[68] D. Baye ,L. Filippin and M. Godefroid : Phys. Rev. **E 84**, 043305.1 (2014).

[69] B. Chakrabarti, T.K. Das and P.K. Debnath : J. Low Temp Phys **157**, 73-81 (2009).

[70] G. Lacroix , C. Semay and F. Buisseret : Phys. Rev. **E 86**(2), 026705.1 (2012).

[71] S. Boffi, M. Bouten, C. Ciofi degli Atti, J. Sawicki : Nucl. Phys. **A 120**, 135.1 (1968).

[72] Al-Jaber S M : Nuovo Cimento **125**, 1099-1108 (2010).

[73] P. Amore and F. M. Fernndez : Int. J. Mod. Phys. src **81**, 045011.1 (2010).

[74] S. Flgge : Practical Quantum Mechanics (Berlin: Springer)(1999).